Monitoring the Variation in Cosmic Muon Rate Using INO-ICAL Prototype Detector

Abhisek Datta,[a] Naba K. Mondal,[b] B. Satyanarayana[b]

[a] *IIT Kharagpur, Kharagpur-721 302, West Bengal*

[b] *Tata Institute of Fundamental Research, Mumbai-400005*

Abstract

RPC is the proposed active detector element in the INO-ICAL experiment. A prototype detector stack comprising of 12 layers of 1 m × 1 m RPCs has been built at Tata Institute of Fundamental Research (TIFR). This detector stack is used as a cosmic muon telescope and it is also a test bench for many other R&Ds. The study of muon counting rate, as continuously monitored by this set up, is presented here.

Introduction

The INO-ICAL is a proposed neutrino physics experiment in India. The proposed detector for the India-based Neutrino Observatory (INO) experiment is Iron CALorimeter (ICAL) where target mass is 50 kton of iron and active detector is RPC to detect charged particles. During the R&D process, a prototype stack of 12 layers of 1 m × 1 m RPCs has been built at TIFR. The stack is running under cosmic ray test for last 3-4 years. Cosmic muons are monitored continuously in this detector stack. The cosmic muon data are analysed on an hourly basis and the counting rate is observed. A variation in the counting rate is noticeable with time and it can be correlated to the change in the atmospheric parameters, viz barometric pressure, temperature etc. A preliminary study, based upon several months of muon data, is presented in this report. A brief description of the detector set-up and the analysis of event data are discussed in the following sections.

Cosmic ray and muons

The muon is an elementary particle similar to the electron, with unitary electric charge and a spin of 1/2. Together with the electron, the tau, and the

three neutrinos, it is classified as a lepton. The muon is an unstable subatomic particle with a mean lifetime of 2.2 μs and has a mass of 105.7 MeV/c^2, which is about 200 times the mass of an electron.

Cosmic Rays primarily consist of protons (90%), alpha particle (9%) and electrons (1%). The highly energetic protons interact with the atmosphere and produce pions and other hadrons(say Kaon etc.). Probability of production of pions is more than other hadrons. These particles are unstable and decay to lighter particles. In these process muons are produced.

$$\pi^- \longrightarrow \mu^- + \bar{\nu}_\mu$$
$$\pi^+ \longrightarrow \mu^+ + \nu_\mu$$

Due to their large mass, energy lost by muons through radiation is very less and it loses energy mainly by ionization, while electron being much lighter than muons lose energy both by radiation and ionization. This allows muons of a given energy to penetrate far more deeply into matter than electrons. This is why penetrating power of muons is more than electrons, and on the earth's atmosphere or even in the underground, muons rate is more than any other lepton.

Pressure and temperature changes in the Earth's atmosphere result in small variations in the muon flux at sea level which are related to the interaction mechanisms of a high energy primary particle passing through a thick layer of air. Amplitude and phase of daily variation are not constant over long periods and may undergo periodic as well as non-periodic variations. Amplitude and phase of the variation also depends on latitude and altitude of the place and acceptance of the detector. Variations of muon flux are also observed due to other events like solar flares and magnetic storms. The investigation of meteorological effect is of special importance to any further study of the cosmic ray variations, since only after the correction for such effects are the measured data able to provide information on the variations due to causes beyond the Earth's atmosphere.

Experimental Setup

A Resistive Plate Chamber (RPC) is a particle detector in which a constant and uniform electric field is applied between two parallel electrode plates, atleast one of which is made of a material with high bulk resistivity. A gas mixture with a high absorption coefficient for ultraviolet light is flown through the gap between the electrodes. Due to the high resistivity of the electrodes,

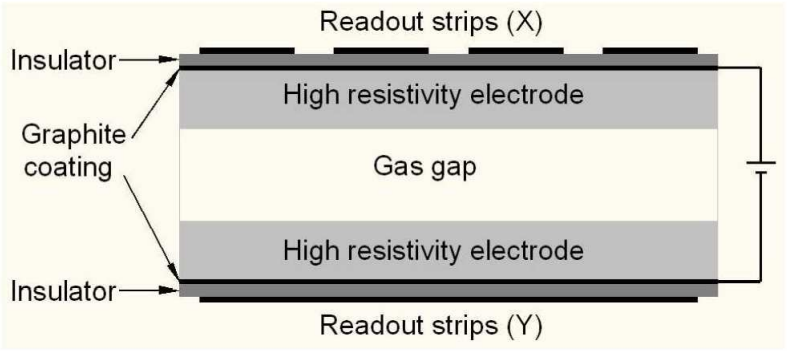

Fig. 1. Resistive Plate Chamber Detector
[1]

the electric field is confined to the area around the point where the discharge occurred, thus preventing it from propagating through the whole gas volume.

Working principle of the RPCs is based on the ionization of the gas when charged particles pass through it producing electron-ion pairs. If the electric field applied is intense enough then further ionisations are produced by the primary electrons. This multiplication mechanism results in a distribution of free charges in the gas which has the characteristic shape of an avalanche. Recombination takes place during this period and photons are produced which can in turn induce secondary avalanches. The regime in which several secondary avalanches are produced causing large amounts of free charge in the gas is called streamer regime. The propagation of the growing number of charges induces a signal on a read out electrode.

A simple configuration of the RPC detector in use here is shown in 1. Two rectangular electrodes of dimensions 1 m $\times$ 1 m made of glass having bulk resistivity of 10^{10}-$10^{12}\Omega - cm$ are spaced by 2 mm. The electrodes are connected to a high voltage power supply to maintain a uniform and intense electric field of around 5 kV/mm in between the plates. The outer layer of the plates is coated with a thin layer of graphite to ensure the uniform application of the high voltage. The electrodes are kept apart by means of small polycarbonate cylindrical spacers having a diameter of around 11 mm and a bulk resistivity greater than $10^{13}\Omega - cm$. The gas mixture consists of SF_6, Isobutane and an electronegative gas like Freon (R134a). SF_6 is used to control streamer. Isobutane absorbs the photons produced by recombination thus preventing formation of further avalanches. Freon serves the purpose of limiting the amount of free charge in the gas. This type of gas mixture is used to prevent the onset of streamers.

Electric pulses generated by the displacement of free charge in the gas is

[1] Design and Characterization Studies of Resistive Plate Chambers, thesis submitted by Satyanarayana Bheesette to IIT Bombay.

induced on metallic strips capacitively coupled to the gap. The strips are mounted on the external surface of the gap. Two different set of strips (called X-strips and Y-strips) oriented in orthogonal directions are arranged on both sides of the detector to obtain measurements along both the axes. The number of X-strips and Y-strips used are 32 each. The width of each strip is 2.8 cm with a gap of 0.2 cm between each strip. The layers are separated by 16 cm which makes the total height of the detector stack around 176 cm.

Signals picked up by RPCs are processed by pre-amplifiers and followed by discriminators. Muon data are saved on the basis of a proper trigger condition. Usually four layers out of twelve layers are used in a coincidence logic unit to produce the trigger. Here, mainly trigger produced by layer nos. 0, 4, 7 and 11 are used for muon rate monitoring. The Data Acquisition System (DAQ) records the event data and monitoring data. Event data contains muon hit position in a layer and its time of arrival on the basis of trigger signal, whereas monitoring data contains individual channel counting rate on a periodic basis.

Analysis of Cosmic Ray Muon Tracks

A display of muon track is shown in the following figures 2–4, before and after the noise cut along with a linear fit to the track.

From figure 2, it can be seen that in many layers more than one strip are hit (on both X and Y side). Some points arise in the hit pattern due to correlated electronic noise. Therefore, data reduction becomes necessary before fitting. X-side and Y-side data are fitted separately. The procedure for data reduction and fitting is described below:

(1) Layers with no hits or with multiplicity greater than 3 are rejected (as in layers 0, 2, 4 & 10 in the X-Z graph of figure 2).
(2) If the multiplicity is 2 or 3, the layer is rejected if there is a gap of one or more strips in between the hits (as in layers 1 & 11 in the X-Z graph of figure 2). Otherwise, the average of the 2 or 3 hits is taken to be the hit position. Figure 3 shows the graphs after this noise elimination.
(3) If the number of layers remaining is less than 4, the entire event is rejected.
(4) If the event is accepted, a linear fit is made to the hit points.
(5) If the residual (|Fit−Hit|) is greater than 1 strip, then the layer is rejected.
(6) After this if the number of layers becomes less than 4, the event is rejected. If the event is accepted another linear fit is made to the hit points, and the results are saved. Figure 4 shows the linear fit to the hit points in both the X-Z and Y-Z planes.

From the linear fitted track, slope and intercept of both the tracks i.e. in the

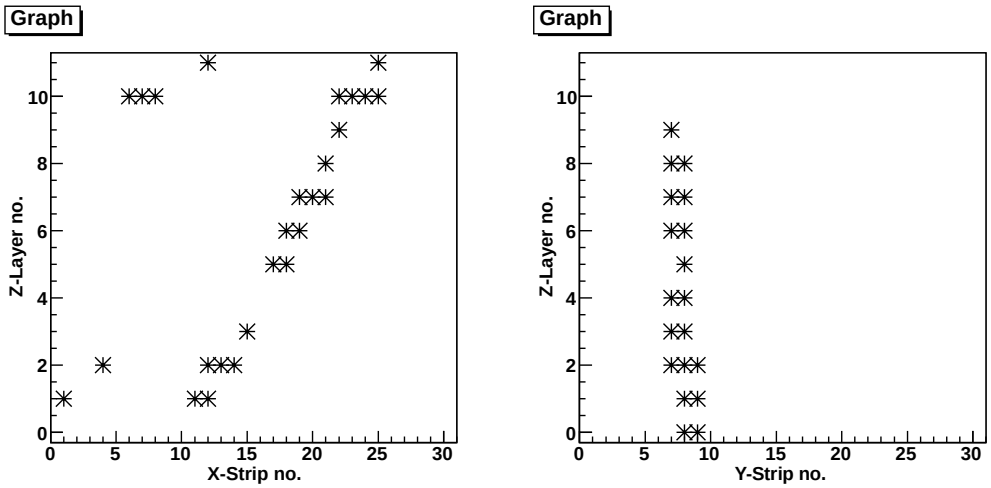

Fig. 2. Cosmic Ray Muon Track before noise elimination

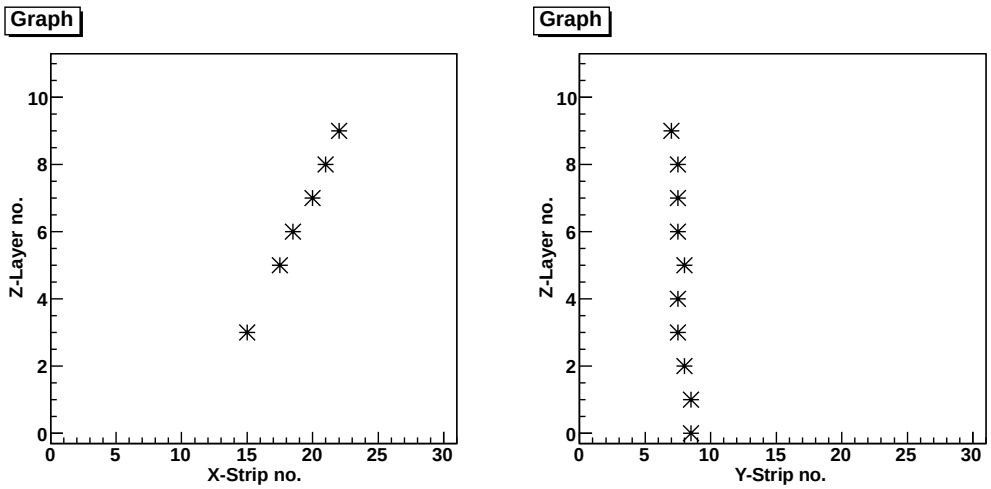

Fig. 3. Cosmic Ray Muon Track after noise elimination

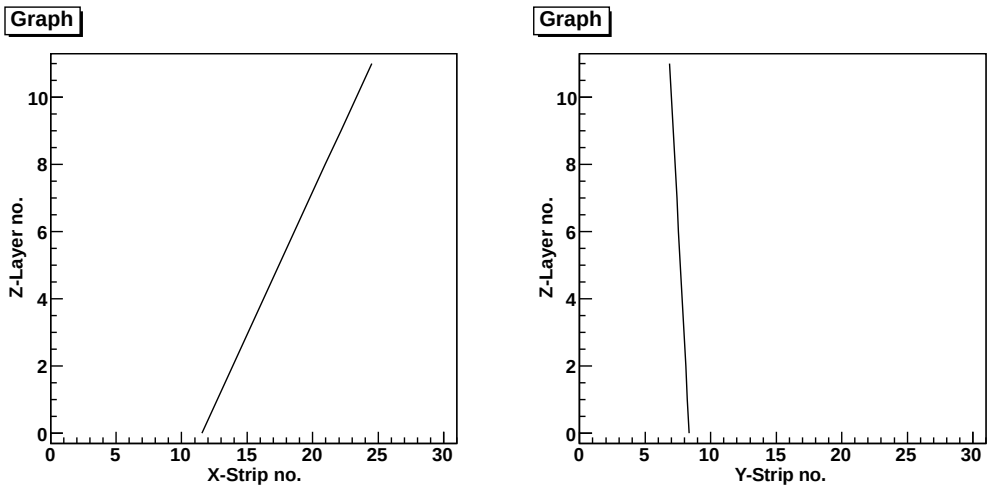

Fig. 4. Cosmic Ray Muon Track after linear fitting

X-Z plane and the Y-Z plane are obtained. The χ^2/ndf distribution is also obtained after the calculation of χ^2/ndf by the following formula.
ndf = number of degrees of freedom = number of data points - number of free parameters

$$\chi^2 = \sum \frac{(r^{expt} - r^{theory})^2}{r^{expt}} \tag{1}$$

r^{expt} = experimental data point

r^{theory} = theoretically predicted data point from linear fit

The events for which the fitted muon track passes through the layers 0,4,7 and 11 are then selected. The reason for imposing this selection is explained in the following section. Then, the events which have a value of χ^2/ndf lying between 0 and 2 are finally selected for calculating the zenith angle of the muon track and included in the zenith angle distribution plot.

Zenith Angle Distribution of Cosmic Muons

As explained in the previous section, the slope and intercept of the fitted tracks in both X-Z and Y-Z plane of all the selected events are calculated. The two graphs only give us projections of the actual muon track in 3 dimensions. From the slope and intercept of both projections the zenith angle i.e. the angle the muon track makes with vertical or Z-axis can be calculated.

Firstly, the total path length l between the plane of the top layer and the plane of the bottom layer is given by

$$l = \sqrt{(x_{11} - x_0)^2 + (y_{11} - y_0)^2 + (z_{11} - z_0)^2} \tag{2}$$

where (x_0, y_0, z_0) are the coordinates in the plane of the bottom layer and (x_{11}, y_{11}, z_{11}) are the coordinates in the plane of the top layer which are estimated from the linear fit.

The value of the zenith angle θ of a track is given by

$$\theta = cos^{-1}(\frac{h}{l}) \tag{3}$$

where h is the stack height and l is the path length

Figure 5 shows the zenith angle distribution of cosmic ray muons for one particular data file which originally contained data of 5,00,000 events spread over a time interval of a little more than 10 hours. The total number of muons detected during this time (after going through the selection procedure explained

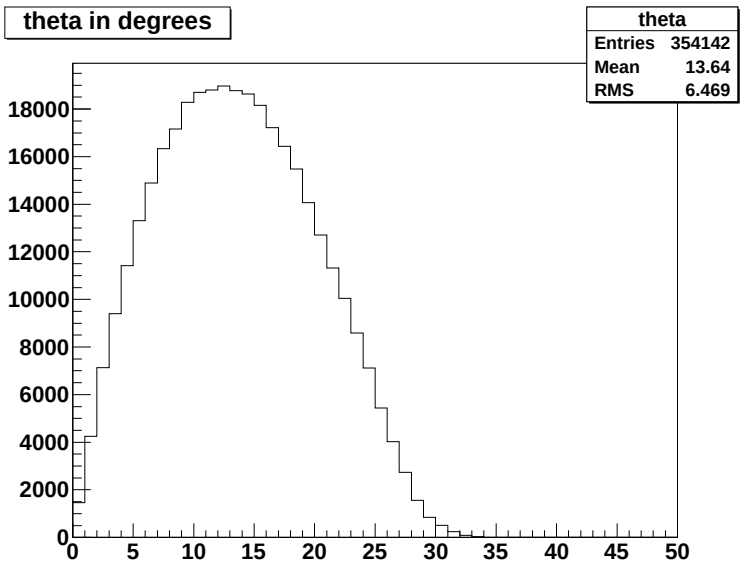

Fig. 5. Zenith Angle Distribution

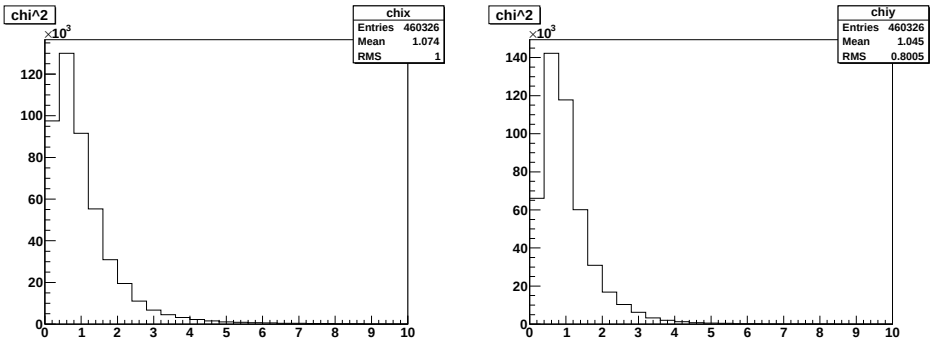

Fig. 6. Chi-square distribution for X-Z and Y-Z linear fits

before) is 3,54,142 as displayed in the figure. Figure 6 shows the chi-square distribution for the X-Z and Y-Z track fits for this file.

In order to scan muon counting rate each event file recorded over several hours is sampled on an hour basis. Figure 7 shows the zenith angle distribution per hour for the same file shown before. For this file, the average number of muon events per hour is 33,433. The number of events in the last histogram is substantially less because the last histogram does not contain data over one complete hour.

The general angular distribution of cosmic ray muons is considered as

$$I_\theta = I_0 cos^n \theta \tag{4}$$

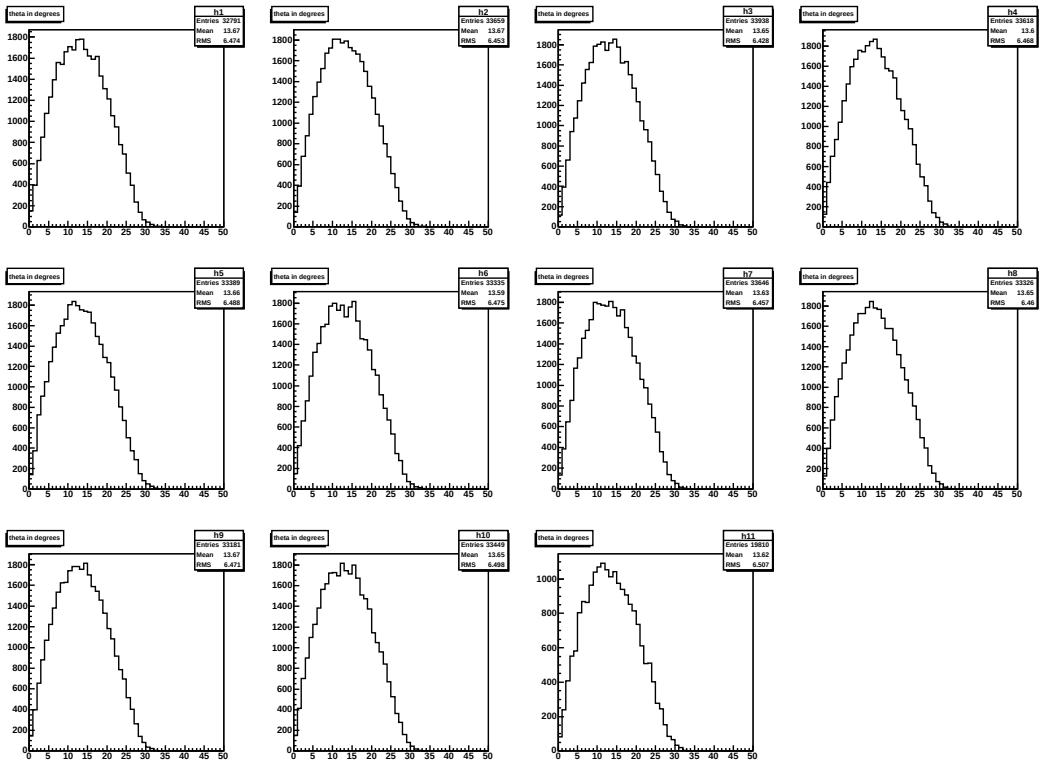

Fig. 7. Zenith Angle Distribution per hour

where I_0 is the vertical intensity ($cm^{-2}sec^{-1}sr^{-1}$)

The exponent n is approximated to be 2 at sea level and in the energy range of muons as mainly detected by this detector. The value of n generally depends on energy of the muons, latitude, altitude etc.

Now, the muon counting rate as detected by the detector, N (number of events/sec) is given as:

$$N_{\theta_1 \to \theta_2} = \int_{\theta_1}^{\theta_2} N(\theta) d\theta = \int_{\theta_1}^{\theta_2} I(\theta) \omega(\theta) d\Omega \tag{5}$$

The observed muon count rate N(θ) thus depends on two factors:-

- The incident atmospheric muon flux which is given by $I_0 cos^2\theta$.
- The combination of trigger layers selected which determines the geometrical acceptance $\omega(\theta)$ of the detector

The geometrical acceptance of the detector $\omega(\theta)$ includes the solid angle factor $d\Omega = sin\theta d\theta d\phi$ which plays a role in determining the shape of the zenith angle distribution along with $I(\theta) = I_0 cos^2\theta$. The factor $sin\theta \to 0$ as $\theta \to 0$ and so the entire distribution tends to 0 as $\theta \to 0$. It also has a peak determined by

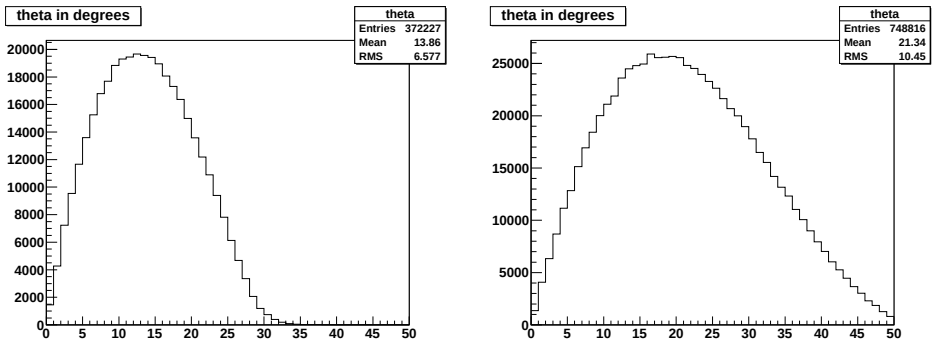

Fig. 8. Zenith Angle Distribution for trigger layers 0,4,7,11 and 0,1,3,4 before imposing the layer condition

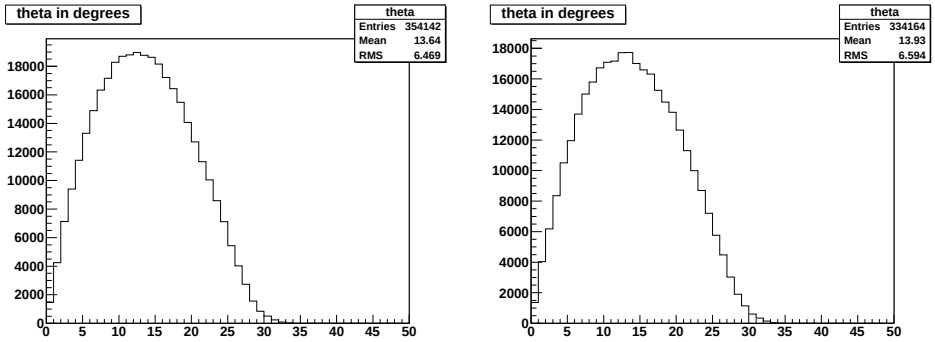

Fig. 9. Zenith Angle Distribution for trigger layers 0,4,7,11 and 0,1,3,4 after imposing the layer condition

the combined effect of the two factors and then falls off to 0 at some value of θ which is determined by the selection of different trigger criteria.

As different trigger criteria changes the detector solid angular acceptance, muon counting rate is going to be different unless a fixed trigger criterion is used. Here in figure 8 results are shown for trigger layer 0,4,7,11 and also for 0,1,3,4 for comparison of the counting rate.

The difference in the width of the distribution is very clear from the figure. Also the average number of muons per hour is significantly different. So in order to study the variation in muon flux solely due to atmospheric and other external factors (like solar flares) only those events should be considered for which the detector acceptance is same. In this case, the most common trigger layer combination used is 0,4,7,11 which is the tightest trigger condition among all the others used. So for all data files (with different trigger layer combinations) an extra condition has been imposed which selects only those events for which the fitted muon track passes through the layers 0,4,7 and 11 in addition to satisfying its respective trigger criterion (during the data acquisition). Figure

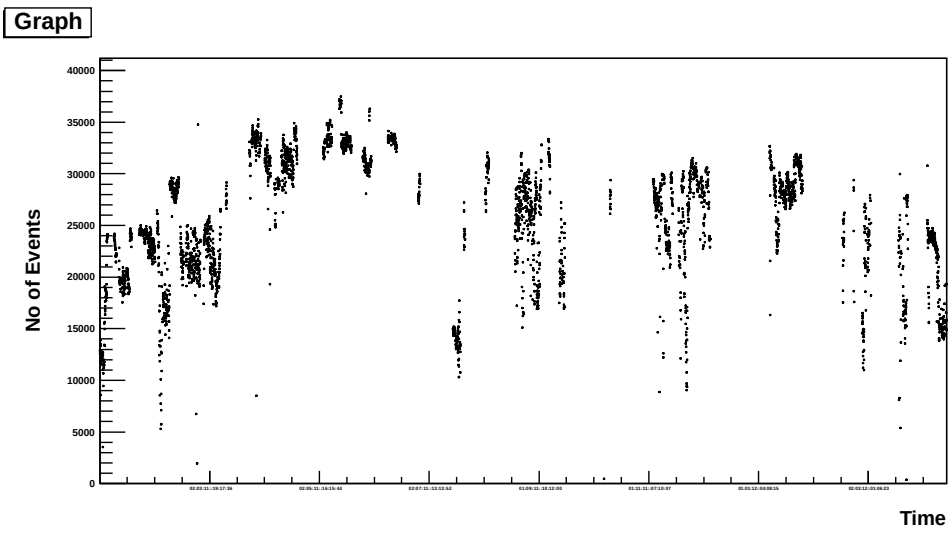

Fig. 10. Variation of Muon Counting Rate with time

9 shows the zenith angle plots of the same data files as shown in figure 8 after imposing this condition. It is observed that now the distribution and count rate are now similar in both cases and thus imposing this condition will make the data sets uniform irrespective of their trigger criteria.

Analysis and Results

As seen in the previous section, the number of muons detected per hour is obtained from the histograms plotted for every hour. This procedure is repeated for all the data files after imposing the extra condition mentioned in the previous section to make the data sets uniform with respect to trigger criteria. Figure 10 shows the plot of the muon counting rate (number of events/hour) against time for all the months in 2011 starting from January and also for January, February, March and April of 2012. There are some gaps in the data sets as seen in the figure. These gaps are due to the fact that data had not been taken during those times due to reasons like detector maintenance etc. Figure 11 shows zoomed in views of the variations in the muon rate at two different times. The periodic nature of the variation is clearly observed in these two figures. Similar diurnal variation can be observed in various regions of the plot. It is also seen from the plot that the count rate has reduced drastically in some areas. This is due to high level of noise which has been observed by monitoring several individual events and also from the rejection % which has been mentioned later.

From the zenith angle distributions, the value of the vertical muon intensity I_0 can be obtained. The variation of I_0 has also been plotted against time and it displays similar kind of variation as displayed by the count rate as shown

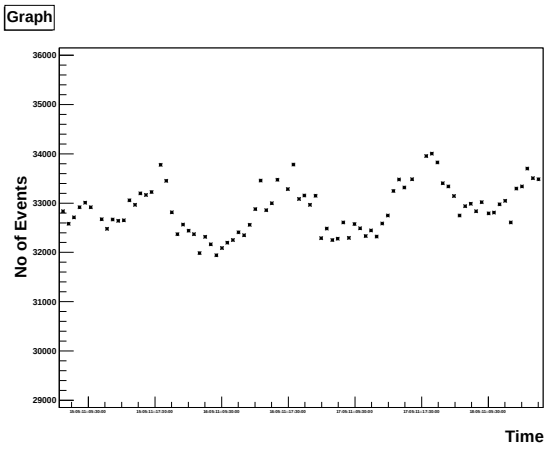

(a) May 2011

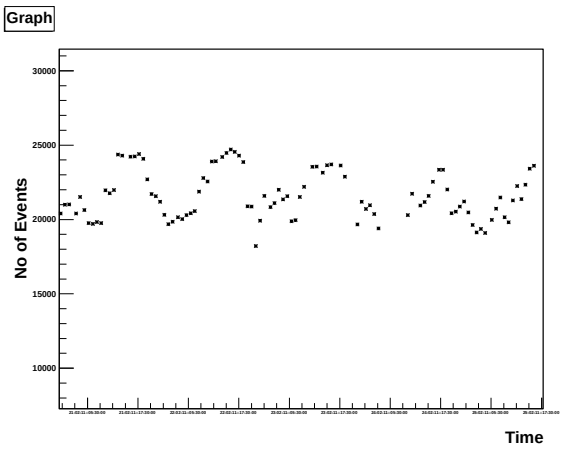

(b) February 2011

Fig. 11. Periodic Nature of Variation in different portions of the plot

in figure 12. The average value of I_0 calculated over the months March-June 2011 comes out to be around $7.72814 \times 10^{-3} cm^{-2} sec^{-1} sr^{-1}$.

The rejection %, one just after noise elimination and the other one after the combined process of noise elimination, chi-square and layer (0,4,7,11) constraints, have also been monitored over the entire data set. This information along with the total number of events recorded and the approximate number of hours of data acquisition for a particular file, gives an indication of the noise level and also the actual trigger criteria present during data acquisition.

The data obtained during the months March-June 2011 are the cleanest with least noise, the rejection % due to noise elimination varying between $7 - 10\%$ only, and the total rejection % being around $28 - 30\%$. This is the reason for

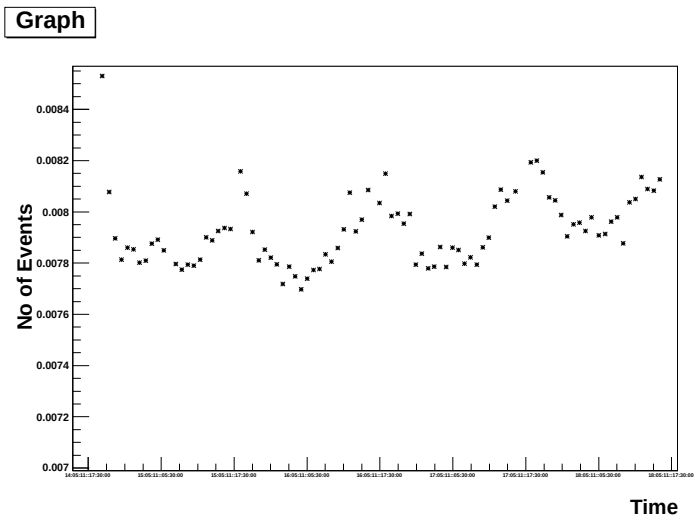

Fig. 12. Variation of I_0 with time

observing such clear diurnal variations during this period especially in May 2011.

A higher value of rejection % may imply two things - higher noise level or a looser trigger criteria than 0,4,7,11. For events with looser trigger criterion, there is more probability of less than 4 points being left in the graphs after layer elimination due to noise and thus leading to rejection of the event. But since for looser trigger, the total number of events recorded is much larger than for the case of tighter trigger, this elimination along with the rejection of events due to layer(0,4,7,11) constraint will finally return a value of muon counts per hour which is consistent with other data sets. For example, for a event with trigger layer combination 7,8,10,11, the rejection % due to noise is 41.71% and the total rejection % is 76.37%. But since the total number of events recorded is much greater than the events with trigger layer combination 0,4,7,11 the count rates values come to be consistent over both.

But during the months December 2010 and January 2011 for example, the noise rejection % is much higher, around 60-70%. This cannot be entirely due to loose trigger but also due to very high noise level. Even noise rejection % around 80-90 % has been observed in some data with very low count rate. It is for this reason data from December 2010 has not been analyzed further. January 2011 is kept in the analysis due to lesser noise level in later parts of the month.

Another observation made was that during October 2011, the count rate was extremely low. This was due to high noise(greater than 50%) and also extremely low value of the total number of events recorded. It has been observed that the zenith angle distribution falls off to 0 at $20^o - 25^o$ during this time

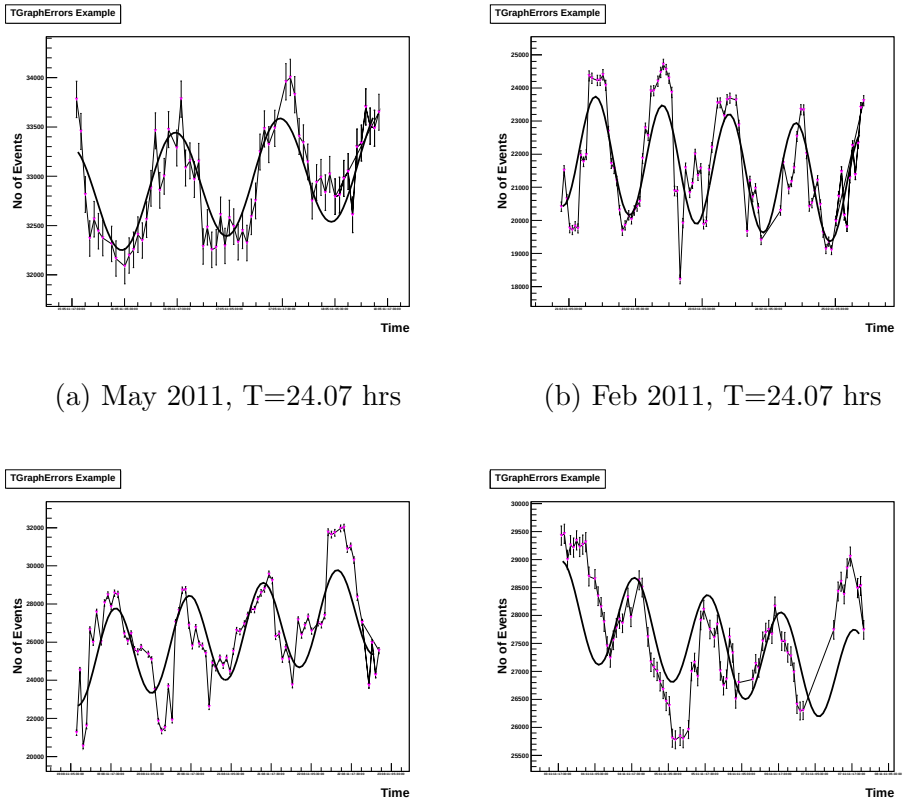

(a) May 2011, T=24.07 hrs

(b) Feb 2011, T=24.07 hrs

(c) Aug 2011, T=22.14 hrs

(d) Nov 2011, T=23.81 hrs

Fig. 13. Fitted Curves to count rate variations

as compared to $30^o - 35^o$ during other times. This has been caused due to a decrease in the solid angular aperture of the detector and a trigger tighter than 0,4,7,11 might be a reason.

The diurnal variations in muon count rate in several portions of the total plot were then fitted independently. The time period of variation were obtained to be around 23-24 hours for the different fits. Figure 13 show the fits to the data points in 4 such portions of the plot. The time of the year and the time period of the fits are mentioned at the bottom of each figure.

It is observed that the fitted curve reaches a maximum at around 5:30 pm in the afternoon and a minimum at around 5:30 am in the morning. This can be correlated to the change in temperature during the day. The temperature increases during the day after 5:30 am and muon count also increases with increase in temperature and reaches a maximum. Again after 5:30 pm, the temperature decreases during the evening and night and muon count also decreases to a minimum. The correlation of muon count rate variation with temperature changes is explained in the following section.

Changes in atmospheric pressure also has effect on the muon count rate, but it is not correlated here in this analysis. Also the significant reduction in the count rate in the months January and February 2011 might have been an effect of large solar flares which had been observed on 24th January, 14th-15th February and also on 24th February. This is only a possibility and there is no confirmation from the analysis performed here.

As explained previously, noise levels are quite high during some time intervals. Due to the presence of such non-uniform noise levels, possible variations over a longer period of time like annual variations are not visible clearly in this plot. There may be a hint of annual variation in the plot with the count rate high during April-June and lower during August-February but the count rate in March and April 2012 again decreased significantly due to high noise level. So this data is not sufficient to conclude about any annual variation. Due to the same reason the plot has not been fitted with any function with time period around 1 year, but independently with 24 hour time periods.

Discussions

Variation of muon rate over different geographical locations, due to atmospheric effects etc. are studied for a long time and many results exist in literature. The atmospheric effects on the muon flux have been mathematically treated and summarized by Dorman in [1].

The parametrized variation of the muon flux with atmospheric factors is given by Dorman as :

$$\frac{\delta C}{C} = k_p \delta h_0 + \int_0^{h_0} W_T(h) \delta T(h) dh \tag{6}$$

where h_0 is the observation level, k_p is the barometric coefficient and $W_T(h)$ are the partial temperature coefficients that characterize the contribution of each atmospheric layer to the total temperature effect.

- Barometric Effects : The barometric effect is always negative i.e. k_p is always negative. This is because high pressure at the observation level results in greater absorption of the μ - component in the air, thus resulting in a lower level of muon flux.
- Temperature Effects: As the temperature increases the density of the atmosphere decreases (at constant pressure). With decrease in density of the atmosphere, the probability of the muon (which is produced in the upper atmosphere) getting absorbed in the atmosphere also decreases thus resulting in increase in the muon flux at the detector level. On the other hand, decrease in temperature leads to increase in density of the atmosphere, and

thus results in greater absorption of the muons, and decrease in muon flux at the detector level.

- External factors : Muon flux is also effected by events like Solar Flares, Coronal Mass Ejection (CME) and Geomagnetic Storms. Sometimes there is a rapid decrease in the galactic cosmic ray intensity following a CME. It occurs due to the magnetic field of the plasma solar wind sweeping some of the galactic cosmic rays away from the Earth. This is termed as a Forbush Decrease.

The net diurnal variation observed can be attributed to the combined variation of pressure and temperature effects. Due to presence of high noise level during some time intervals, annual or any other variation of muon count rate over long period of time could not be observed. But good fits obtained to diurnal variations in several regions of the plot indicate that it may be possible to observe some kind of annual variation with cleaner data, if the detector is run uniformly, under stable conditions over a long period of time. Since the noise level was least in the data acquired during May-June 2011 using layers 0,4,7,11 as the trigger criteria, this can be taken up as the trigger criteria for the detector operation for this kind of study.

Conclusion

This project has thus covered the analysis of cosmic muon data from the prototype detector stack. The muon counting rate was monitored for all the months of 2011 and January, February, March and April of 2012, and it was observed to display a diurnal variation. This variation was understood to be due to a combined effect of pressure and temperature changes. Similar analysis of data obtained by running the RPC detector stack uniformly under stable conditions over a long period of time may show other variations over longer period of time like annual variations and also variations due to external factors like solar flares.

Acknowledgment

I would like to thank my project guide Prof. Naba K. Mondal and Dr. B. Satyanarayana for their kind helps, suggestions and guidelines during my work. I would also like to thank Prof Gobinda Majumder, Sumanta Pal and Deepak Samuel for guiding me and providing great help during the programming processes, and also for the understanding of the experimental setups and the detectors. I would like to express my gratitude to the Indian Academy of

Sciences Summer Project Programme, the Visiting Students Research Programme (VSRP), Tata Institute of Fundamental Research and its Department of High Energy Physics (DHEP) for giving me this opportunity to work in this place and its laboratories, interact with such eminent scientists, and for this wonderful exposure to the various aspects of research in both theoretical and experimental physics. Collaborative efforts from other group members are also highly acknowledged.

References

(1) L. Dorman, Cosmic Ray Variations, State Publishing House (Moskow), 1957.
(2) M. Bertaina, L. Briatore, A.Longhetto, G.Navarra AND EAS-Top Coll, The atmospheric muon flux in correlation with temperature variations in the low stratosphere (50-200 mb), ICRC (Moskow), 2007
(3) Design and Characterization Studies of Resistive Plate Chambers, thesis submitted by Satyanarayana Bheesette to IIT Bombay.
(4) INO Report INO/2006/01